SEWAGE SLUDGE-DERIVED ADSORBENTS FOR H_2S REMOVAL

Andrey Bagreev, Svetlana Bashkova, David C. Locke[1], and Teresa J. Bandosz
Department of Chemistry, The City College of New York and the Graduate School of the City University of New York, New York, N Y 10031
[1]Department of Chemistry Queens College, CUNY, Flushing, N Y 1136

Introduction

Various methods have been used to dispose of or utilize municipal sewage sludge (1), including incineration, landfilling, road surfacing, conversion to fertilizer, compression into building blocks, and carbonization (1-4). Since 1976 several patents have been issued on carbonization of sewage sludge and various applications of the final materials (4-7). Carbonization of sludge in the presence of chemical activating agents such as zinc chloride and sulfuric acid produces new sorbents, with patented applications in such processes as removal of organics in the final stages of water cleaning (5) and removal of chlorinated organics (6).

The process of carbonization of biosolids has been studied in detail using different chemical agents and various conditions (8-11). Materials obtained as a result of the treatment have surface areas between 100 and 500 m^2/g, but their performance as adsorbents has been demonstrated to be much worse than that of activated carbons. The ability of these adsorbents to remove organics such as phenols, or sulfur dioxide and hydrogen sulfide (10, 11) have been tested so far; their capacity for the adsorption of SO_2 reported by Lu was less than 10% of the capacity of Ajax activated carbon (11). When the performance for H_2S adsorption was compared, the capacity of sludge-derived adsorbents was only 25% of the capacity of Calgon carbon, IVP 4x6 (10).

The objective of this paper is to demonstrate the superior performance of materials obtained by simple carbonization of the New York City municipal sewage sludge-derived product, Terrene®, as adsorbents for hydrogen sulfide. As indicated elsewhere (12), this sludge-derived material is expected to work well as a hydrogen sulfide adsorbent because of the presence of either iron and other catalytic metals, or organic nitrogen in the matrix of the carbonaceous components. The results obtained show that the capacity of these adsorbents exceeds that of coconut shell-based activated carbon, which is considered as one of the alternative sorbents to replace the caustic-impregnated carbons commonly used as hydrogen sulfide adsorbents in municipal sewage treatment plants (13, 14).

Experimental

Materials

Terrene® was obtained from the New York Organic Fertilizer Company, (Bronx, New York) in the form of 3 mm diameter granules with about 5% water content. It contains around 35% inorganic matter mainly in the form of iron, alumina, silica oxides and carbonates and 60% of organic matter. The adsorbents studied were prepared by pyrolysis of Terrene® at temperatures between 400-950ºC in a nitrogen atmosphere in a fixed bed (horizontal furnace). The heating rate was 10 ºC/min and holding time 60 min. The samples are referred to as SC400, SC600, SC800 and SC950 where numbers represent the pyrolysis temperatures of 400, 600, 800 and 950 ºC, respectively. For comparison, the experiments were done using the as-received carbon manufactured from coconut shells by Watelink Barnabey and Sutcliffe, S208. The sorbent is produced in the form of 6.4 x 3.2 mm pellets. To provide the same dynamic conditions of the experiment, S208 carbon was granulated and the fraction with the same size (1-3 mm) as the carbonized Terrene® was chosen for the breakthrough experiments.

To study the effect of iron, a 20 g subsample of the S208 carbon was impregnated with 40 ml ferric chloride (5%). The sample was then hydrolyzed in the presence of dilute sodium hydroxide, filtered, and dried. The material was then heated under the same conditions as SC950 (950 ºC). The sample is referred to as S208-Fe.

The prepared materials were studied as hydrogen sulfide adsorbents in the dynamic tests described below. After exhaustion of its adsorbent capacity, each sample is identified by adding the letter "E" to its designation (it indicates for exhaustion).

Methods

The dynamic tests were carried out at room temperature to evaluate the capacity of sorbents for H_2S removal. Adsorbent samples were packed into a column (length 60 mm, diameter 9 mm, bed volume 6 cm^3) and prehumidified with moist air (relative humidity 80 % at 25 ºC) for an hour. The amount of adsorbed water was estimated from the increase in the sample weight after

prehumidification (the sorbents were removed from the column and weighted). Moist air (relative humidity 80 % at 25 ºC) containing 0.3 % (3000 ppm) H_2S was then passed through the column of adsorbent at 0.5 L/min. The elution of H_2S was monitored using an Interscan LD-17 H_2S continuous monitor system interfaced with a computer data acquisition program. The test was stopped at the breakthrough concentration of 500 ppm. The adsorption capacities of each sorbent in terms of g of H_2S per gram of carbon were calculated by integration of the area above the breakthrough curves, and from the H_2S concentration in the inlet gas, flow rate, breakthrough time, and mass of sorbent.

Nitrogen adsorption isotherms were measured using an ASAP 2010 analyzer (Micromeritics, Norcross, GA, USA) at -196 ºC. Before the experiment the samples were degassed at 120 ºC to constant pressure of 10^{-5} torr. The isotherms were used to calculate the specific surface area, S_{DFT}; micropore volume, V_{mic}; and pore size distribution using Density Functional Theory (DFT) (15, 16). The relative microporosity was calculated as the ratio of the micropore volume to the total pore volume. In addition, BET surface area, S_{BET}, and the total pore volume, V_t (evaluated from the last point of the isotherm) were calculated.

Chemical charter of the surface was characterized by the pH of carbon suspension in water. A 0.4 g sample of dry adsorbent was added to 20 mL of deionized water and the suspension stirred overnight to reach equilibrium. The sample was filtered and the pH of solution was measured using an Accumet Basic pH meter (Fisher Scientific, Springfield, NJ, USA).

Thermal analysis was carried out using TA Instruments Thermal Analyzer (New Castle, DE, USA). The heating rate was 10 ºC/min in a nitrogen atmosphere at 100 mL/min flow rate.

Results and Discussion

The calculated H_2S breakthrough capacities are summarized in Table 1. Each measurement was done at least twice and the capacities represent the mean values. It is clearly seen that with increasing pyrolysis temperature the capacity of the sludge-derived adsorbents is significantly increased. It is remarkable that the capacity of the sample treated at 950 ºC, SC950, is twice that of the as received activated carbon. The materials obtained are mainly basic in their chemical nature. The ability of samples to retain water was also studied. As indicated elsewhere (17-19), the presence of water on activated carbons contributes to the dissociation of hydrogen sulfide and facilitates to its oxidation to sulfur and sulfur dioxide (14, 17-21). The proposed mechanism involves 1) H_2S adsorption on the carbon surface, 2) its dissolution in a water film, 3) dissociation of H_2S in an adsorbed state in the water film , 4) surface reaction with adsorbed oxygen with formation of elemental sulfur 4a) or sulfur dioxide 4b), and 5) further oxidation of SO_2 to H_2SO_4 in the presence of water (14, 20, 21).

$$H_2S_{gas} \xrightarrow{K_H} H_2S_{ads} \quad (1)$$

$$H_2S_{ads} \xrightarrow{K_S} H_2S_{ads\text{-}liq} \quad (2)$$

$$H_2S_{ads\text{-}liq} \xrightarrow{K_a} HS^-_{ads} + H^+ \quad (3)$$

$$HS^-_{ads} + O^*_{ads} \xrightarrow{K_{R1}} S_{ads} + OH^- \quad (4a)$$

$$HS^-_{ads} + 3\,O^*_{ads} \xrightarrow{K_{R2}} SO_{2\,ads} + OH^- \quad (4b)$$

$$SO_{2ads} + O^*_{ads} + H_2O_{ads} \xrightarrow{K_{R3}} H_2SO_{4\,ads} \quad (5)$$

$$H^+ + OH^- \longrightarrow H_2O \quad (6)$$

where H_2S_{gas}, $H_2S_{ads\text{-}liq}$, and H_2S_{ads} correspond to H_2S in gas, liquid and adsorbed phases, respectively; K_H, K_S, K_a and K_{R1} , K_{R2} , K_{R3} are equilibrium constants for related processes (adsorption, gas solubility, dissociation, and surface reaction constants); O^*_{ads} is dissociatively adsorbed oxygen, S_{ads} , SO_{2ads} , $H_2SO_{4\,ads}$ represent sulfur, SO_2 and H_2SO_4 as the end products of the surface oxidation reactions.

In the case of the sludge-derived materials, the mechanism of hydrogen sulfide removal probably differs from that for activated carbons. For the activated carbons, the significant decrease in the adsorption capacity corresponding to exhaustion is usually caused by the formation of sulfuric acid (14, 22). For the sludge-derived samples, only a small decrease in pH is observed and after exhaustion the materials preserve their basic pH. As was pointed out elsewhere (14, 21, 22), for conventional carbons, basic initial pH favors the formation of elemental and polymeric sulfur as the final products of oxidation; there is a threshold pH below which this process becomes infeasible. However, this rule probably does not apply to our sludge-derived materials.

For the sludge derived materials the mechanism of H_2S adsorption-oxidation in wet conditions may be more complex due to the presence both carbonaceous matter and different forms of metal oxides and carbonates. Hence at least two types of active sites may exist on these materials: one - on the surface of porous carbon and second – on the surface of metal oxides or carbonates. It is likely that the reaction of H_2S oxidation occurs on the carbon and oxides surfaces simultaneously with formation of elemental

sulfur, metal sulfides and sulfuric acid which later reacts with carbonates.

The possibility of chemisorption in the process of H_2S removal on sludge-derived carbon was also pointed out by Lu and Lau; however, the capacity of their adsorbent was reported to be only 25% of that of activated carbon chosen for a comparison (10). A remarkably good performance of the SC950 carbon as a hydrogen sulfide adsorbent also indicates that differences in the mechanisms of the process exist within the series of materials, probably attributable to changes in their chemical and structural composition.

Table 1. pH of the materials studied, their H_2S breakthrough capacities, and the quantity of water adsorbed during prehumidification.

Sample	pH	H_2S breakthrough capacity (mg/g)	Water adsorbed (mg/g)
SC400	7.9	8.2	60
SC400E	7.5	---	---
SC600	11.4	14.9	40
SC600E	9.2	---	---
SC800	11.2	23.6	48
SC800E	8.8	---	---
SC950	10.8	82.6	62
SC950E	9.9	---	---
S208	10	48.8	77
S208E	7.4	---	---
S208-Fe	7.4	104.5	165
S208-FeE	2.0	---	---

The demonstration of the superiority of the performance of the sludge-derived adsorbents would not be complete without the detailed analysis of the pore structure and its comparison to coconut shell based activated carbon. Structural parameters calculated from nitrogen adsorption isotherms are given in Table 2. As discussed elsewhere (12), the surface area and pore volumes increase with increasing carbonization temperature. It is noteworthy that there are no significant differences in the porosity of SC800 and SC950, which could explain the differences in their H_2S adsorption capacity. This supports our hypothesis that significant changes in surface chemistry favorable to H_2S chemisorption occur when the sludge is pyrolyzed at 950 °C.

After H_2S adsorption/oxidation, the surface areas and pore volumes significantly decreased. This decrease is especially apparent in the volume of micropores indicating that they are active in the adsorption/oxidation process. Assuming that sulfur is the oxidation product deposited in these pores, the volume of deposited sulfur (density assumed to be 2 g/cm^3) can be calculated based on the amount of hydrogen sulfide adsorbed. The values are presented in Table 2 as V_{sulf}. For samples obtained at 800 °C and lower temperatures the volume of sulfur is much smaller than the decrease in the pore volume suggesting either the blockage of the pore entrances or the presence of other sulfur compounds such as sulfides on the surface. On the other hand, for the SC950E sample the decrease in the micropore volume (and the total pore volume) is less than the calculated volume of sulfur. This indicates not only that all the pores of this material are completely filled with sulfur but that sulfur must be also chemisorbed on the surface in the form of chemical compounds.

Differences in the mechanism of the hydrogen sulfide immobilization before and after impregnation with iron are seen from an analysis of the structural parameters obtained for the coconut shell-based samples (Table 2). It is interesting that the surface area and pore volumes slightly increased after impregnation with iron oxide, suggesting a contribution of the iron deposit to porosity development. After H_2S adsorption on the initial sample, the volume of micropores decreased only 0.007 cm^3/g, much less than the calculated volume of sulfur deposited on this carbon (0.023 cm^3/g). This finding indicates that in this case sulfur is adsorbed in the mesopores. After treatment with iron a significant decrease in the volume of micropores is found. Since this decrease is almost three times larger than the calculated volume of sulfur, the deposited species must block the entrances to the micropores as was observed for some sludge-derived samples.

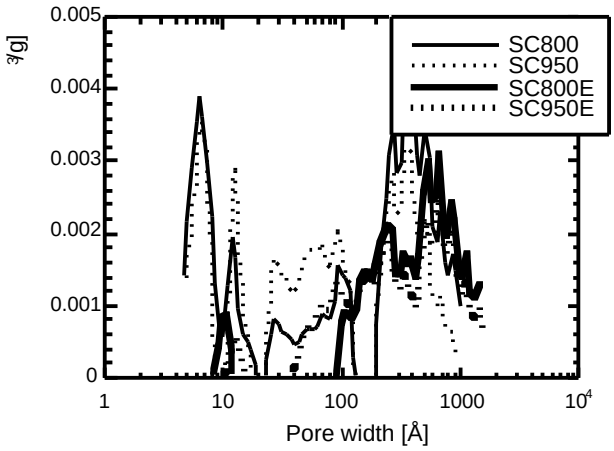

Figure 1. Pore size distributions for sludge derived samples before and after H_2S adsorption.

Detailed changes in microporosity caused by hydrogen sulfide adsorption/oxidation are seen from the analysis of the pore size distributions (PSD) presented in Figure 1.

PSD's were calculated using density functional theory (15, 16). For the initial samples development of small pores is observed with increasing heat treatment temperature. All the sludge-derived samples have a significant development of mesoporosity as a result of the presence of inorganic matter (12). It is probable that microporosity exists in the carbonaceous deposit (around 30% of total mass of the adsorbent) or/and on the interface between carbon and inorganic matter. It is clearly seen that after H_2S adsorption almost all the micropores disappear; the volume of mesopores decreased but not as drastically as the volume of micropores. A similar result is found for the acid-treated samples.

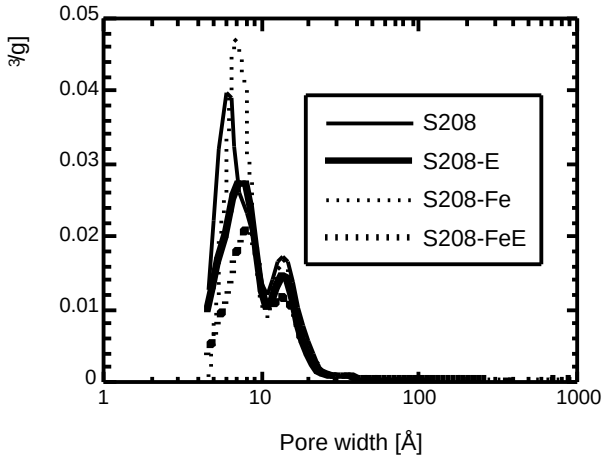

Figure 2.
Changes in pore size distributions for S208 series of samples before and after H_2S adsorption.

Similar trends were observed for activated carbons in which even after exhaustion a significant volume of micropores was still available for nitrogen adsorption (14, 20-22). Indeed, this is noticed for the S208 carbon before and after impregnation with iron (Figure 2). If the "catalytic efficiency" of this carbon for hydrogen sulfide immobilization was similar to that of SC950, its capacity would be much higher because of the larger pore volume. Unfortunately, this is not the case even after impregnation with iron.

Differences in the performance of the materials studied are visualized in the bar diagram (Figure 3) which presents the specific capacity (capacity divided by surface area, in mg/m^2) versus the thermal treatment temperature. The diagram clearly shows that for all sludge-derived carbons except SC950, the performances of each are similar, suggesting that the mechanism of immobilization is similar. The performance of the acid treated samples except SC950 is also similar. The exception of the SC950 sample supports the hypothesis that catalytic centers are formed at 950 °C. For comparison, the specific capacities of the S208 and S208-Fe samples are 0.05 mg/m^2 and 0.19 mg/m^2, respectively. These low values clearly demonstrate the superiority of the surface features of the sludge-derived SC950 adsorbent crucial for hydrogen sulfide adsorption/oxidation.

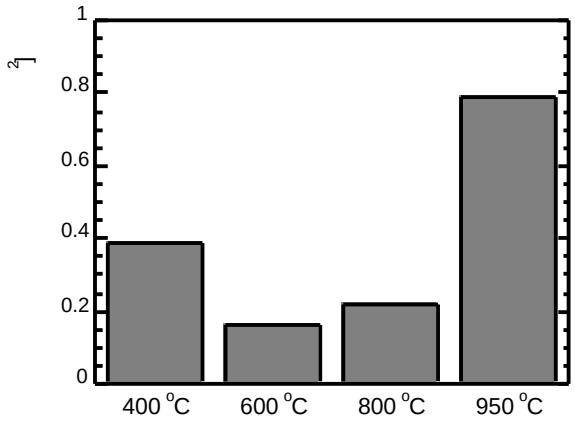

Figure 3.
Specific H_2S adsorption *vs* temperature of heat treatment.

As discussed elsewhere (14, 20, 22), when activated carbons are used as hydrogen sulfide adsorbents, H_2S is oxidized to either sulfur or sulfuric acid. The presence of sulfuric acid is demonstrated by the low temperature peak in the DTG curves (between 200-300° C), and the presence of sulfur by the peak centered at about 400 °C (14, 20-24). Usually a good correlation is found between the amount of hydrogen sulfide adsorbed on an activated carbon and the amount of species determined using thermal analysis. However, applying the same approach to the sludge-derived materials revealed a significant discrepancy between the amount of sulfur adsorbed and that detected using the TA method. The results are summarized in Table 3 and Figure 4. Although for some of our samples the two peaks representing sulfur and sulfur dioxide are present, the amount of sulfur as these species was only 20% to 50 % of the total sulfur adsorbed. The SO_2 peak is well defined (with a shoulder representing sulfur) only for the SC950E sample. This suggests that heating to 950°C caused the changes in surface chemistry and porosity that enhanced the selectivity for oxidation of H_2S to SO_2.

Failure to account for all the sulfur deposited on the surface suggests that new species are formed whose decomposition temperatures are higher than the 1000°C used in our experiment. Even if we assume that FeS_x is a reaction product in the form of troilite (FeS, melting point:

1193-1200 °C) or pyrite (FeS_2, melting point: 1171 °C) its DTG peak should appear at temperatures as high as 1200 °C (25). Indeed, when the SC950E sample was heated to 1300 °C the intensity of a peak centered between 1000 °C and 1200 °C almost doubled (Figure 6). Although this temperature is higher than the sludge carbonization temperature, such a significant increase in intensity indicates the formation of new species as a result of exposure to hydrogen sulfide. If other catalytically active metals are present their sulfur compounds are expected to be even more thermally stable. Since the presence of SO_2 in the effluent gas was checked experimentally and eliminated as a possibility, the only conclusion we can draw at this stage of our study is that sulfur chemically bonds to metal oxides present in the mineral-like forms. A detailed study of this hypothesis is in progress.

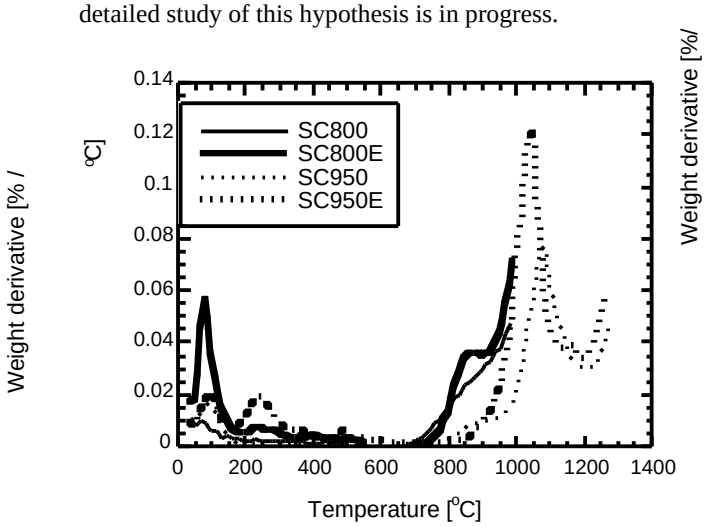

Figure 4.
DTG curves in nitrogen for the sludge-derived adsorbents and their acid-treated counterparts.

The presence of iron also affects the selectivity of oxidation of H_2S on the S208 carbon. After iron impregnation, more sulfuric acid is formed (Figure 7) as demonstrated by the significant decrease in pH (Table 2) and the increase in the intensity in the DTG peak at about 230 °C. Also supporting the significant role of iron in the selectivity of H_2S oxidation for the S208-FeE sample is the only slight increase in the intensity of the peak assigned to sulfur. As a result of surface modification more H_2S was adsorbed and all of it was converted to sulfur dioxide.

Conclusions

Based on the data presented above, the sludge-derived adsorbent, SC950, has superior capacity for hydrogen sulfide adsorption. It performs much better than the coconut shell-based microporous carbon adsorbents currently under consideration as alternatives to caustic-impregnated carbons in sewage treatment plants. On the surface of the sludge-derived adsorbent, hydrogen sulfide is immobilized mainly in the form of sulfur compounds resulting from interactions of H_2S with mineral-like metal oxides containing iron, zinc, copper, and/or others. Under our experimental conditions the capacity of the best sludge-derived adsorbents is exhausted when all pores are filled with the oxidation products.

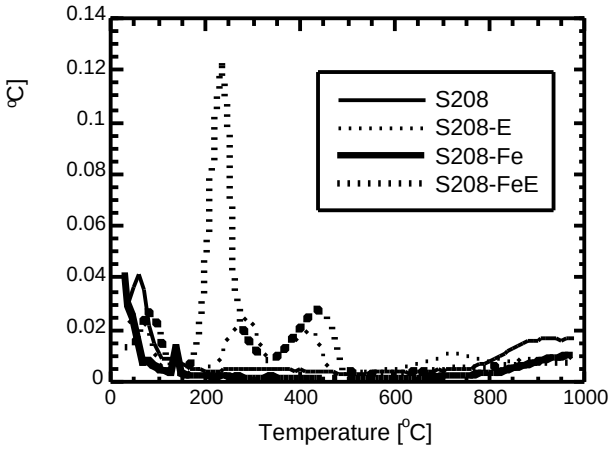

Figure 5.
DTG curves in nitrogen for the S208 series of samples.

Acknowledgment
This study was supported by CUNY Collaborative Research grant #91906.

References

1. Manahan SE. Environmental Chemistry, 6th ed.; CRC Press: Boca Raton, FL, 1994.
2. Biosolid Generation, Use, and Disposal in The United States: EPA530-R-99-009, September 1999; www.epa.gov.
3. Sutherland J. US Patent 3,998,757 (1976).
4. Nickerson RD, Messman HC. US Patent. 3,887,461 (1975)
5. Lewis FM. US Patent 4,122,036 (1977).
6. Kemmer FM, Robertson RS, Mattix RD. US Patent 3,619,420 (1971)
7. Abe H, Kondoh T, Fukuda H, Takahashi M, Aoyama T, Miyake M. US Patent 5,338,462 (1994).
8. Chiang PC, You JH. Can. J. Chem. Eng. 1987; 65: 922.

9. Lu GQ, Low JCF, Liu CY, Lau AC. Fuel 1995; 74: 3444.
10. Lu GQ, Lau DD. Gas Sep. Purif. 1996; 10: 103.
11. Lu GQ. Environ. Tech. 1995; 16: 495.
12. Bagreev A, Locke DC, Bandosz TJ. Carbon, in press.
13. Bandosz TJ, Bagreev A, Adib F, Turk A. Environ. Sci. Technol. 2000; 34: 1069.
14. Adib F, Bagreev A, Bandosz TJ. Environ. Sci. Technol. 2000; 34: 686.
15. Lastoskie CM, Gubbins KE, Quirke N. J. Phys. Chem. 1993; 97: 4786.
16. Olivier JP. J. Porous Materials 1995; *2*: 9.
17. Hedden K, Huber. L, Rao BR. VDI Bericht 1976; 37: 253.
18. Meyoo V, Trimm DL. J. Chem. Tech. Biotechnol. 1997; 68: 411.
19. Meyoo V, Lee JH, Trimm DL, Cant NW. Catalysis Today 1998; 44: 67.
20. Adib F, Bagreev A, Bandosz TJ. J. Coll. Interface Sci. 1999; 214: 407.
21. Adib F, Bagreev A, Bandosz TJ. J. Coll. Interface Sci. 1999; 216: 360.
22. Adib F, Bagreev A, Bandosz TJ. Langmuir 2000; 16: 1980.
23. Rodriguez-Mirasol J, Cordero T, Rodriguez JJ. Extended Abstracts of 23rd Biennial Conference on Carbon, College Park, July 1997 p. 376.
24. Chang CH. Carbon 1981; 19: 175.
25. Handbook of Chemistry and Physics, 67th ed.,Weast, R.C. Ed. CRC press, Boca Raton, Fl, 1986.

Table 2. Structural parameters calculated from nitrogen adsorption isotherms and estimated hypothetical sulfur volume (assuming density equal to 2 g/cm^3).

Sample	S_{BET} (m^2/g)	S_{DFT} (m^2/g)	V_{mic} (cm^3/g)	V_t(0.995*) (cm^3/g)	V_{mic}/V_t	ΔV_{mic} (cm^3/g)	ΔV_t (cm^3/g)	V_{sulf} (cm^3/g)
SC400	41	21	0.006	0.075	0.080			
SC400E	12	8	0.003	0.057	0.053	0.003	0.018	0.004
SC600	99	92	0.030	0.115	0.261			
SC600E	14	9	0.001	0.040	0.025	0.029	0.075	0.007
SC800	104	106	0.033	0.107	0.308			
SC800E	14	9	0.003	0.064	0.047	0.030	0.043	0.013
SC950	122	104	0.028	0.100	0.280			
SC950E	21	13	0.002	0.065	0.031	0.026	0.035	0.039
S208	880	889	0.359	0.457	0.786			
S208E	781	774	0.352	0.414	0.850	0.070	0.043	0.023
S208-Fe	933	932	0.406	0.498	0.815			
S208-FeE	560	528	0.243	0.294	0.827	0.163	0.204	0.049

*at the relative pressure p/p_o equal to 0.995.

Table 3. Weight loss (%) at the temperature ranges related to the presence of the products of H_2S oxidation and estimated amount of sulfur from breakthrough capacity test ($S_{B.Th}$) and thermal analysis (S_{TA})

Sample	150-350 ºC	350-500 ºC	500-700 ºC	S_{TA}	$S_{B.Th.}$
SC400	3.38	---	---	---	---
SC400E	2.57	---	---	N/A	0.77
SC600	1.73	1.83	---		
SC600E	2.19	1.61	---	0.23	1.14
SC800	0.47	0.23	0.82		
SC800E	1.05	0.56	0.49	0.62	2.22
SC950	0.12	0.01	0.07		
SC950E	2.62	1.05	0.08	3.73	7.76
S208	1.01	0.79	---		
S208E	2.42	1.94	---	1.86	4.58
S208-Fe	0.34	0.17	---		
S208-FeE	7.57	2.78	---	6.23	9.81